International Journal of Engineering &Technology, 7 (4) (2018) 7021-7027

International Journal of Engineering & Technology

Website: www.sciencepubco.com/index.php/IJET
doi: 10.14419/ijet.v7i4.16825
Research paper

Performance of photovoltaic pumping station using a centrifugal motor-pump working at fixed speed

Eric Simonguy [1] *, Eric Korsaga [1], Jean M'boliguipa [2], Toussaint Tilado Guingané [1], Zacharie Koalaga [1]

[1] *Laboratory of Materials and Environment (LAME), University Joseph Ki-Zerbo 03 BP 7021 Ouagadougou 03, Burkina Faso*
[2] *Carnot Laboratory of Energetic (LEC), University of Bangui, Central African Republic*
**Corresponding author E-mail: simonguy_eric@yahoo.fr*

Abstract

The work presented in this paper studies the performances of a direct coupled photovoltaic (PV) pumping system such as the water storage is carried out indirectly in a tank. The centrifugal pump is driven by a squirrel cage Asynchronous Motor (AM) fed by three-phase voltage inverter using a Pulse Width Modulation (PWM) swictching technique. The strategy of Boost converter command by Proportional-Integral (PI) controller is used to feed the motor-pump with constants voltage and frequency. The simulation results in Matlab/Simulink software show that, on the one hand, the dynamic performances of the motor pump depend of the rotor inertia moment (or mechanic power) and on the other hand, the evolution of the water volume is not affected by the rapid variations of illumination.

Keywords: *PV Pumping System; Centrifugal Motor-Pump; Fixed Speed; Modeling; PI Controller; Dynamic Performance*.

1. Introduction

The use of the solar energy for pumping water is particularly well adapted to the rural areas and isolated sites. The increasing demand of water in these zones made that a growing interest is done to the utilization of photovoltaic (PV) generator as energy source for several motor-pumps. In fact, the realization of autonomous, reliable pumping systems with a good efficiency, gives a practical and economical solution to the water lack problem in desert regions [1].

The majority of the pumping systems now currently established use as electric actuator the Direct Current (DC) motor or the Alternative Current (AC) motor, particularity the cage asynchronous motor [2].

The cage asynchronous motor based on PV pumping systems offers an alternative for a more reliable and maintenance free system [3]. It is much used in the industry and the transport. It is appreciated for its robustness, its weak cost of purchase and maintenance, but its command is in contrary more difficult to realize than for the others electrics machines.

Many strategies have been developed to make it an efficient machine, even in the commanded systems. In general, the driving mode of cage asynchronous motor is divided into two classes, such as:

- The drive at fixed speed;
- The drive at variable speed by using of linked techniques to the scalar control or vectorial command [4].

The drive at variable speed by cage asynchronous motor allows to get the controllable dynamic performances with an optimal efficiency and to realize the energy saving contrary to the drive with fixed speed. But the purchase cost of such equipment for variable speed is more significant, because it is necessary to include the cost of the feeding, the command and the sensors. So we have retained for this work as driving mode, the drive at fixed speed.

This work is organized in two sections: the first section is devoted to the modeling of the system and the second gives the whole of simulation works allowing to analyze the performance of the studied installation.

2. System modeling

The water pumping system considered is composed by a photovoltaic array constituted with 26 branches of 8 modules series-connected, a boost converter with his Proportional-Integral (PI) command, a three-phase voltage inverter, a centrifugal motor-driven pump and a water storage tank. Its synoptic diagram is presented in the following figure:

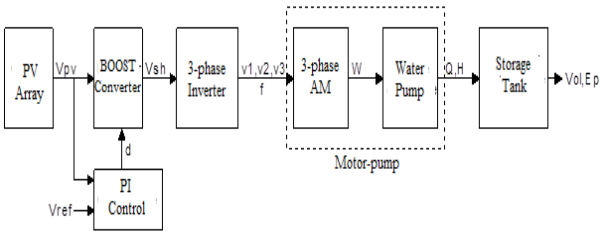

Fig. 1: Synoptic Diagram of the System.

2.1. PV array model

As indicated above, a PV array is composed of a several modules connected in series and in parallel, themselves constituted of PV cells. Many models of PV cells are used in the literature [5], [6]. Among which, the simplest is the single diode model [7 - 11] (Figure 2). It will be used in this study because it provides fairly accurate results.

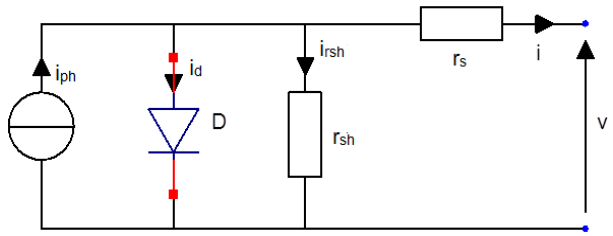

Fig. 2: PV Cell Model.

According to the Kirchoff law, equation (1) is obtained:

$$i = i_{ph} - i_s\left[\exp\left(\frac{q(v+ir_s)}{aKT_C}\right) - 1\right] - \frac{v+r_s i}{r_{sh}} \quad (1)$$

Where i and v are respectively the photodiode current and voltage, i_{ph} is the photocurrent, i_s is the reverses saturation current, r_s is the series resistance, r_{sh} is the parallel resistance, a is diode ideality factor, K is the Boltzmann constant ($1.3854\ 10^{-23}$ J/K) and q is the electron charge ($1.602\ 10^{-19}$ C).
The PV module is obtained by replacing each cell by its equivalent model, for the same illumination and temperature of cells. The equation of the voltage-current characteristic of the PV module is given by (2).

$$I = I_{ph} - I_s\left[\exp\left(\frac{q(V+IR_s)}{aKT_C}\right) - 1\right] - \frac{V+R_s I}{R_{sh}} \quad (2)$$

With

$$I_{ph} = n_p \cdot i_{ph},\ I_s = n_p \cdot i_s,\ R_s = \frac{n_s}{n_p}\cdot r_s,\ R_{sh} = \frac{n_s}{n_p}\cdot r_{sh} \quad (3)$$

Where I_{ph}, I_s, R_s and R_{sh} are respectively the photocurrent, the reverses saturation current, the series resistance and the parallel resistance of the PV module. n_s and n_p are respectively the number of series and parallels connected cells.
The simulation of the model in Standard Test Condition (STC) allows to compare the characteristics of manufacturer (Table 1) and the ones provide by the model.

Table 1: Data Sheet Parameters of JS180W-36M Module

Maximum Power at STC (P_{max})	180 W
Voltage at MPP (V_{pm})	35.14 V
Current at MPP (I_{pm})	5.12 A
Open circuit voltage at STC (V_{co})	43.2 V
Short-circuit current at STC (I_{cc})	5.48 A
Number of cells (n_{cell})	72

Fig. 3 presents the simulated I-V and P-V characteristics of JS180W-36M module of "ENERGIES VERTES Innovation" manufacturer.

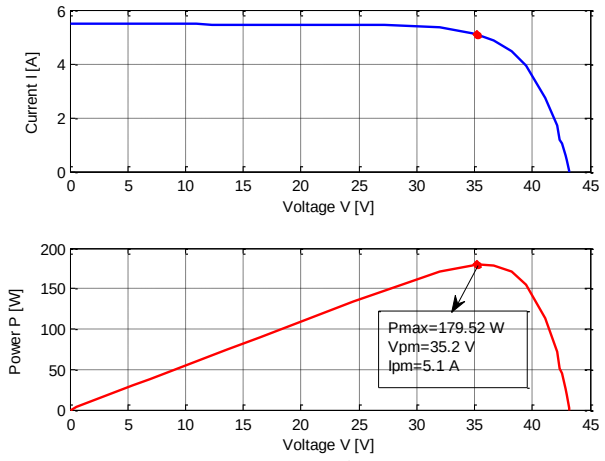

Fig. 3: I-V and P-V Curves of PV Module Model.

At the end of the simulation, we notice that the characteristics of the PV module model are near of these given by the manufacturer. Therefore, the model is retained for the following study.

2.2. Boost converter and his control

The boost converter is needed to efficiently convert a Direct Current (DC) voltage from a lower level to a higher level [11]. It's much used in photovoltaic applications [12], [13], particularly in the solar pumping. The rigorous control of its duty ratio (d) allows to optimize the photovoltaic power by forcing it to work at the maximum of the P-V characteristic. Its electric diagram is presented in Fig. 4.

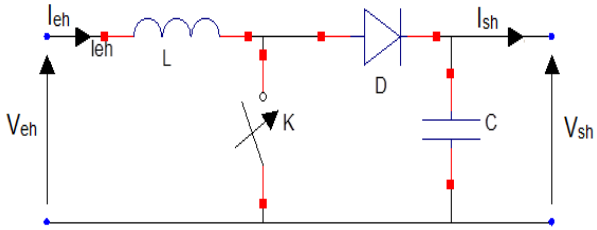

Fig. 4: Boost Converter Scheme.

By using the simplified model, the input value and the output value are related to the duty ratio (d) by the following expression [14], [15]:

$$V_{sh} = \frac{V_{eh}}{1-d} \quad (4)$$

$$I_{sh} = (1-d)\cdot I_{eh} \quad (5)$$

Where V_{eh} and V_{sh} are respectively the input voltage and the output voltage of the converter; I_{eh} and I_{sh} are respectively the input current and the output current.

- Proposed control strategy of the converter

So as to manage the transfer of energy between the PV source and the voltage inverter, the boost converter is controlled in voltage with à Proportional-Integral (PI) regulator. This regulator allows to obtaining very satisfactory results to carry out the voltage control of the boost converter.
The schematic block diagram of converter control is shown in Fig. 5.

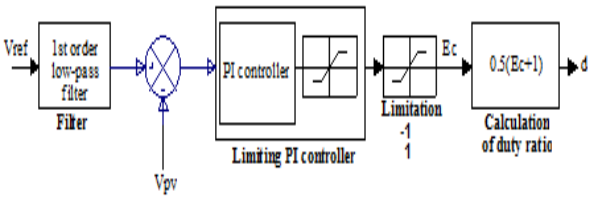

Fig. 5: Boost Converter Control Strategy.

The signal Ec is determine by proportional-integral treatment between the reference voltage V_{ref} and the photovoltaic array voltage V_{pv}. The Limitation block is used to limit the value of Ec between -1 and 1 and the last block calculates the duty ratio value (d).
The PI regulator parameters are determined by the simulation. They are given in Table 2.

Table 2: PI Regulator Parameters

Proportional gain (K_p)	0.004
Intégral gain (K_i)	13
Time-constant of filter (τ)	10^{-4} s

2.3. Inverter model

The function of the inverter is to provide a three-phase alternative voltage to the centrifugal motor-pump from the continuous voltage delivered by the boost converter.

To model the inverter, we will consider that the electronic switches are ideal and operating in complementary regimes which have two states possible and the switching are carried instantaneously.
In considering the medium point 0 of the continuous source as reference point, the voltages v_{m0} (m = a, b, c) take the value $V_{cc}/2$ when the superior switch placed on one arm is in conduction and respectively $-V_{cc}/2$ when the inferior switch placed on the same arm is in conduction [16], [17]. So we get:

$$v_{m0} = \frac{S_m \cdot V_{CC}}{2}, m = a, b, c \quad (6)$$

Where S_m is the command functions of the inverter arms and $S_m = \pm 1$ (state of the switch).
Fig. 6 gives the diagram of the inverter power part (with the continuous source divided in two parts).

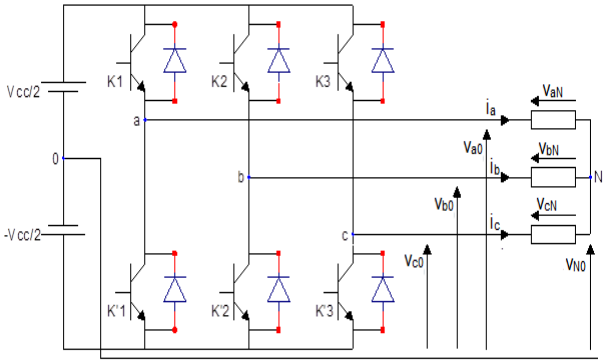

Fig. 6: Inverter Scheme with Continuous Source Divided in Two Parts.

The line to neutral output voltages of the inverter can write under the following form [18]:

$$\begin{cases} v_{aN} = \frac{V_{CC}}{6} \cdot (2.S_a - S_b - S_c) \\ v_{bN} = \frac{V_{CC}}{6} \cdot (2.S_b - S_c - S_a) \\ v_{cN} = \frac{V_{CC}}{6} \cdot (2.S_c - S_a - S_b) \end{cases} \quad (7)$$

Where V_{cc} is the continuous voltage; S_a, S_b et S_c are the command functions of the inverter arms.
The harmonics contained in the output voltages are naturally filtered at fundamental frequency (f=50 Hz) by the motor itself.
In order to obtain the voltage supply of the asynchronous motor in a two-phase system (d, q), the Park's transformation is used.

$$\begin{bmatrix} V_{sd} \\ V_{sq} \end{bmatrix} = [P(\theta)] \begin{bmatrix} v_{aN} \\ v_{bN} \\ v_{cN} \end{bmatrix} \quad (8)$$

Where (v_{aN}, v_{bN} and v_{cN}) are the three-phase voltages supply given by the inverter; (V_{sd}, and V_{sq}) are the d and q axis components of the stator voltage and $[P(\theta)]$ is the Park matrix given by:

$$[P(\theta)] = \frac{2}{3} \cdot \begin{bmatrix} cos(\theta) & cos\left(\theta - \frac{2\pi}{3}\right) & cos\left(\theta - \frac{4\pi}{3}\right) \\ -sin(\theta) & -sin\left(\theta - \frac{2\pi}{3}\right) & -sin\left(\theta - \frac{4\pi}{3}\right) \end{bmatrix} \quad (9)$$

2.4. Motor pump model

2.4.1. Asynchronous motor model

The asynchronous machine is presented by a model brought back to a system of axis d, q, obtained by a Park transformation of a three-phase system into a two-phase system, in a reference frame turning at the synchronism speed [19], [20].
The voltage equations of the asynchronous machine in the (d, q) axis systems are given as follows:

$$\begin{cases} V_{sd} = R_s I_{sd} + \frac{d\emptyset_{sd}}{dt} - \omega_s \cdot \emptyset_{sq} \\ V_{sq} = R_s I_{sq} + \frac{d\emptyset_{sq}}{dt} + \omega_s \cdot \emptyset_{sd} \\ 0 = R_r I_{rd} + \frac{d\emptyset_{rd}}{dt} - (\omega_s - \omega) \cdot \emptyset_{rq} \\ 0 = R_r I_{rq} + \frac{d\emptyset_{rq}}{dt} + (\omega_s - \omega) \cdot \emptyset_{rd} \end{cases} \quad (10)$$

Where (V_{sd}, V_{sq}), (I_{sd}, I_{sq}) and (I_{rd}, I_{rq}) are respectively the Park's components of the stator voltage, the stator current and the rotor current; R_s and R_r are respectively stator resistance and rotor resistance; Φ_{sd} and Φ_{sq} are Park's components of the stator flux, Φ_{rd} and Φ_{rq} are the Park's components of the rotor flux, ω_s and ω are respectively stator pulsation and mechanic pulsation.
The Park components of stator flux are given by the following equations:

$$\emptyset_{sd} = L_s \cdot I_{sd} + M_{sr} \cdot I_{rd} \quad (11)$$

$$\emptyset_{sq} = L_s \cdot I_{sq} + M_{sr} \cdot I_{rq} \quad (12)$$

Where L_s and M_{sr} are respectively the stator inductance and the mutual inductance between the stator and the rotor.
And those of rotor flux are given by:

$$\emptyset_{rd} = L_r \cdot I_{rd} + M_{sr} \cdot I_{sd} \quad (13)$$

$$\emptyset_{rq} = L_r \cdot I_{rq} + M_{sr} \cdot I_{sq} \quad (14)$$

Where L_r is rotor inductance.
The expression of electromagnetic torque is given by:

$$C_{em} = p \cdot M_{sr} \cdot (I_{rd} \cdot I_{sq} - I_{rq} \cdot I_{sd}) = p \cdot \frac{M_{sr}}{L_r} \cdot (\Phi_{rd} \cdot I_{sq} - \Phi_{rq} \cdot I_{sd}) \quad (15)$$

Where p is the pair pole's number.
The statoric and rotoric pulsations are linked by the following equation:

$$\omega_s = p \cdot \Omega + \omega_r \quad (16)$$

Where Ω is the angular velocity of rotation (rd/s).
To generate the complete model of the machine, it is necessary to associate with the electric and electromagnetic equations, the mechanic equation (17).

$$J \cdot \frac{d\Omega}{dt} + f \cdot \Omega = C_{em} - C_r \quad (17)$$

Where C_r and C_{em} are respectively resistant and electromagnetic torques, f is the coefficient of viscous friction and J is the inertia moment of motor.

2.4.2. Centrifugal pump model

The model of the centrifugal pump is based on the similitude laws [21], [22] associated to the equation of the resistant torque that oppose the pump to the motor.
Knowing the performances of a centrifugal pump (Q_n, H_n and P_n) for a rotational speed N_n given, the similitude laws allow to determine the performances (Q, N, and P) for a speed N using the following relationships:

$$Q = Q_n \cdot \left(\frac{N}{N_n}\right), \quad H = H_n \cdot \left(\frac{N}{N_n}\right)^2, \quad P = P_n \cdot \left(\frac{N}{N_n}\right)^3 \quad (18)$$

Where Q and Q_n are the water flow(m^3/h) respectively corresponding to the speed N and N_n, H and H_n are the manometric height respectively corresponding to N and N_n, P and P_n are the mechanic power (kW) respectively corresponding to N and N_n.
The load torque of the centrifugal pump can be described by (19).

$$C_r = k\Omega^2 \quad (19)$$

Where k is the pump torque coefficient (Nm/ (rad/s)^2) and Ω the angular velocity of rotation (rd/s).

2.5. Storage tank model

The aim of the storage tank model is to calculate the volume of the water stocked during the pumping phase.
In fact, a mass of water M stocked in a tank to the height Z_1 allows to realize a work, called potential energy, expressed by the following relation:

$$E_p = MgZ_1 \quad (20)$$

With:

$$M = \rho \cdot Vol = \rho \cdot S \cdot H \quad (21)$$

Where g is the gravity acceleration equal to 9,80 m/s^2, Z_1 is the altitude of the tank support (compared to the soil), ρ is the water density (kg/m^3), Vol is the water volume, S is the section of the tank and H is the water height.
The water volume in the tank is related to the pumping flow Q as:

$$Vol(t) = \int_0^t Q(t)\,dt + Vol_0 \quad (22)$$

Where t is the simulation time (seconds) and Vol_0 is the water reserve. For this study, Vol_0 is fixed at 16 m^3.

3. Simulation results

Fig. 7 presents the complete model of the proposed pumping system implemented in Matlab/Simulink.

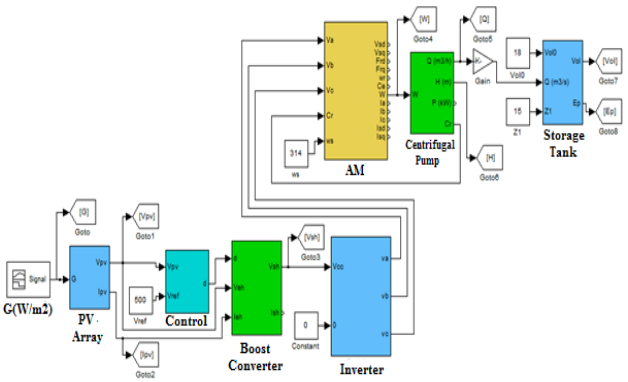

Fig. 7: Matlab/Simulink Model of PV Pumping System.

To study the performances of the system during meteorological disturbances, one applies to the entry the illumination profile of Figure 8. The operating temperature is considered constant and equal to 25ºC.

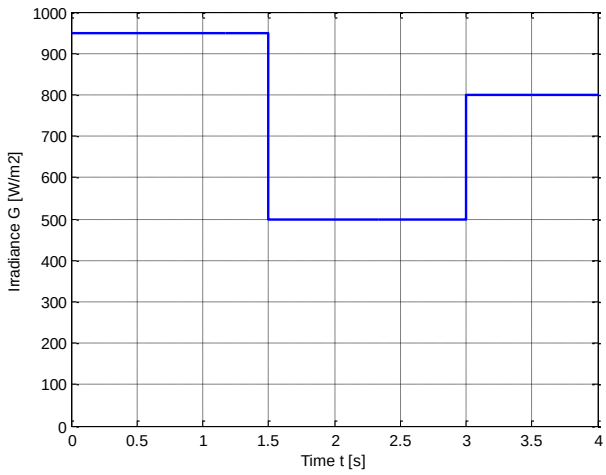

Fig. 8: Illumination Profile.

Simulations are realized for two values of the rotor inertia moment (J). Referring to the data sheet of the manufacturer Leroy Somer [23], the value of J=0.005 kg.m^2 corresponds to a 2 poles asynchronous motor of nominal power equal about to 5 kW and J=0.5 kg.m^2 corresponds to the same asynchronous motor of nominal power equal about to 100 kW. Thus, the rotor inertia moment increases with the motor mechanic power.
The simulation results for two values of J are presented on the following figures:

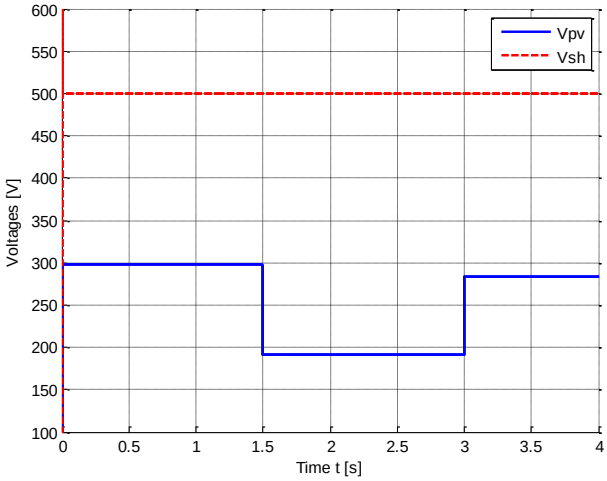

Fig. 9: PV Array Voltage Compared to the Boost Converter's Output Voltage for a Reference Voltage $V_{ref.}$ = 500 V.

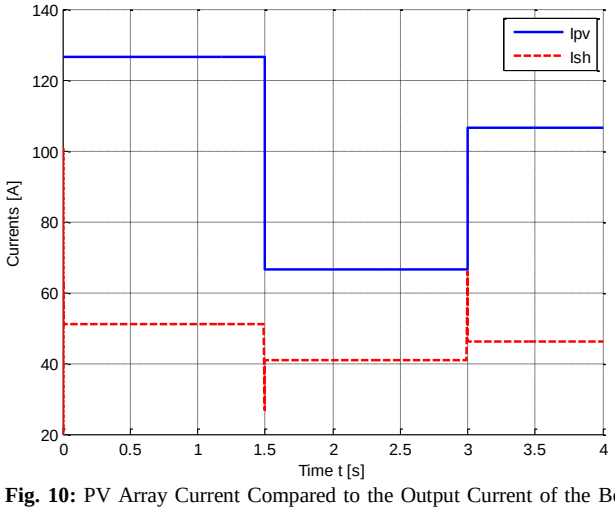

Fig. 10: PV Array Current Compared to the Output Current of the Boost Converter.

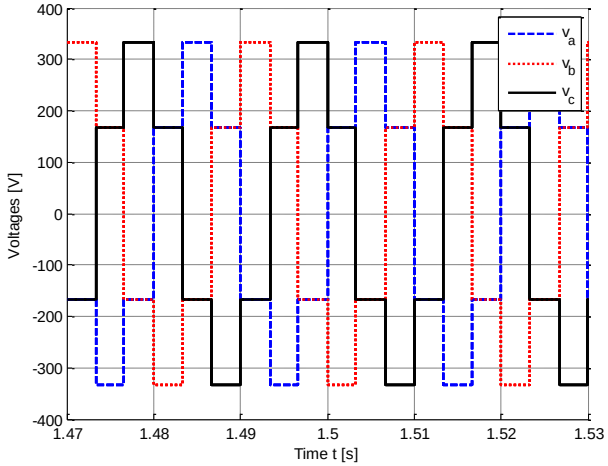

Fig. 11: Output Voltages of Tree-Phase Inverter.

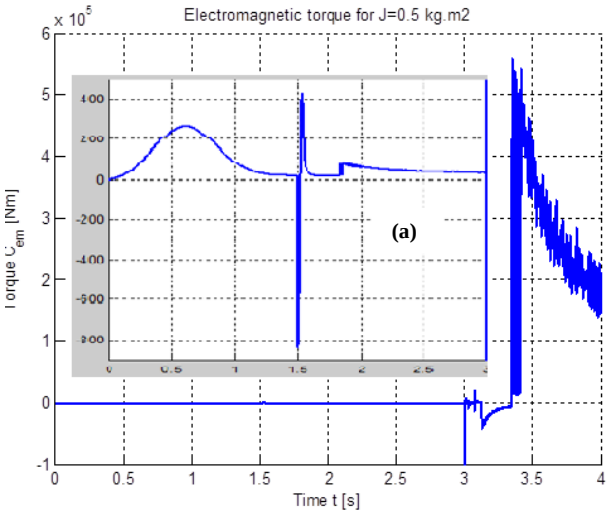

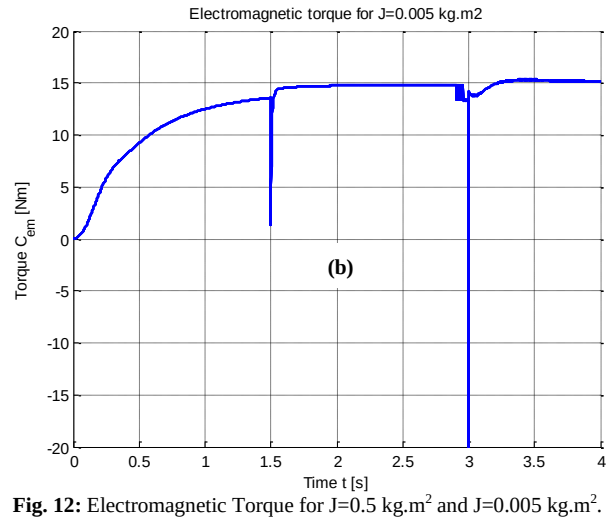

Fig. 12: Electromagnetic Torque for J=0.5 kg.m^2 and J=0.005 kg.m^2.

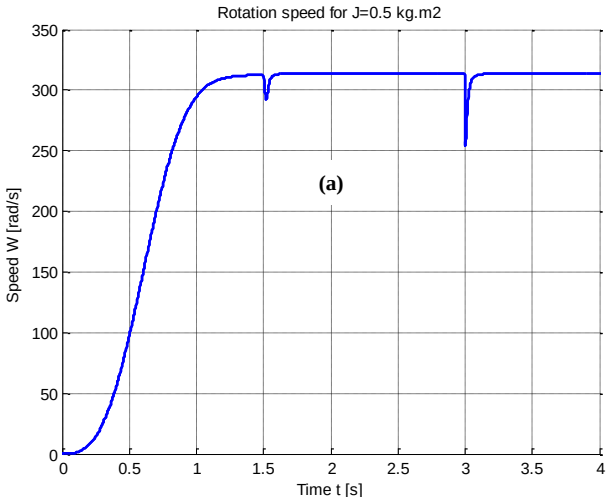

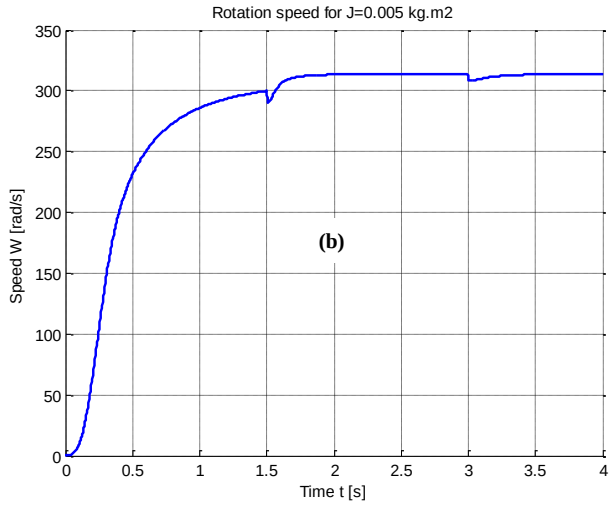

Fig. 13: Rotation Speed for J=0.5 kg.m^2 and J=0.005 kg.m^2.

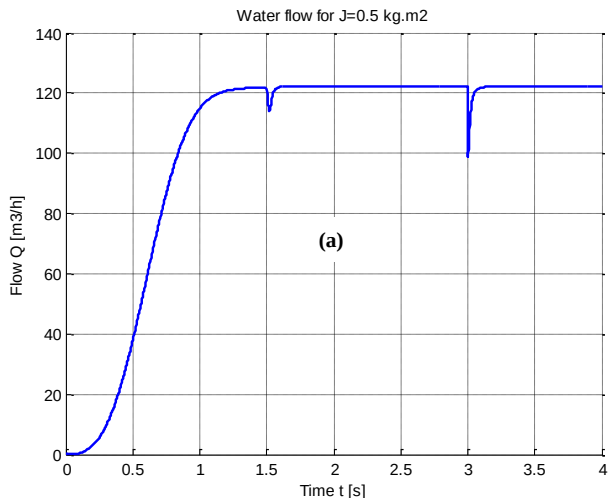

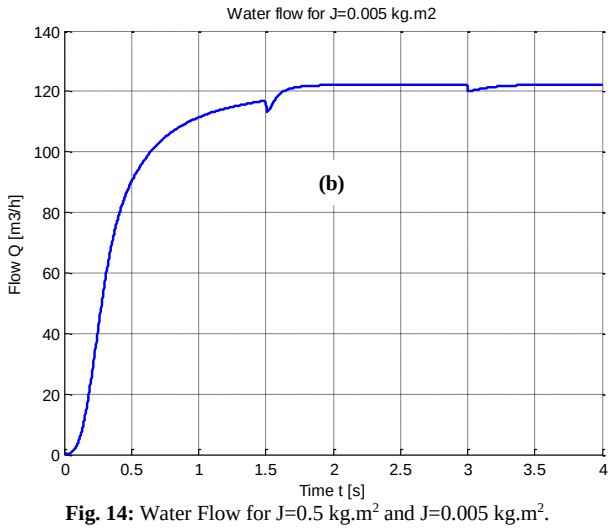

Fig. 14: Water Flow for J=0.5 kg.m^2 and J=0.005 kg.m^2.

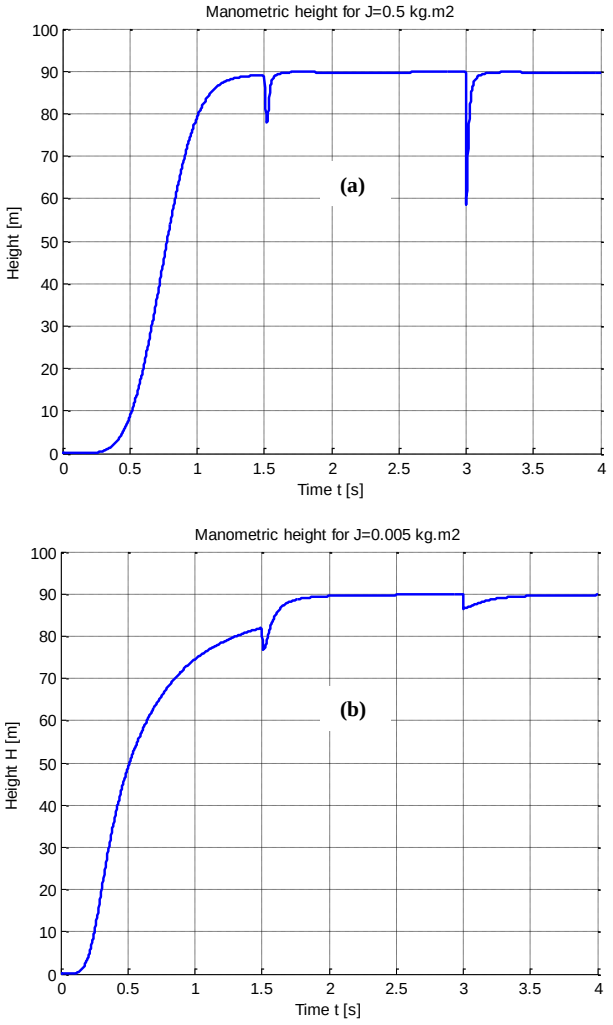

Fig. 15: Manometric Height for J=0.5 kg.m^2 and J=0.005 kg.m^2.

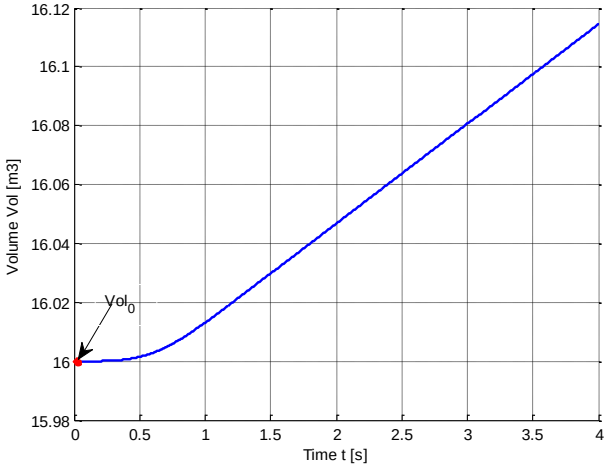

Fig. 16: Water Volume in the Tank.

Fig. 9 and Fig. 10 show the answers of the PV array and the boost converter to a sudden variation of illumination. It proves that the variation of illumination influences the current and the voltage of the PV array. However, the boost converter's output voltage is maintained constant and equal to the reference voltage V_{ref}, showing thus the efficiency of the PI regulator.

Fig. 11 presents the waves of voltage delivered by the three-phase inverter around the first point of illumination change. The magnitudes of the simple voltages are constant, equal to 325 V and their frequencies are equal to 50 Hz.

Fig. 12 presents the electromagnetic torque for two values of the rotor inertia moment (J). For great values of J (Fig. 12 (a)), the torque profile is very demanding: its transitory variations at the different points of changing of illumination are very large and are followed of disturbances, that induces very significant variations of the motor feeding currents, the noise and mechanic vibrations. These constraints brought by the transitory torque tire the driving shaft of the motor-driven pump and heat the windings of the stator. For weak values of J (Fig. 12 (b)), the response of the torque doesn't comprise any more disturbances and never exceeds the nominal torque value (15 N.m). It's also notices that the transitory variations of the torque during the changing of illumination are very weak. That reduces largely the electric and mechanic constraints received by the motor-driven pump.

Fig. 13 presents the rotation speed for two values of J. The rise of speed is faster for great values of J (Fig. 13 (a)). However, one notices at the moments t=1.5 s and t= 3 s the transient drops of speeds to the different points of illumination changes. These transitory variations of speed are very large for the great values of J and small for weak values of J (Fig. 13 (b)). So, for small values of J, the illumination variations disturb weakly the stabilization of speed to its optimal value.

Fig. 14 and Fig. 15 present the flow and the manometric height of the pump respectively for two values of J. They prove that the illumination variations influence weakly the stabilization of the flow and manometric height to their optimal values for the weak values of J (Fig. 14 (b) and Fig. 15 (b)). However, for great values of J (Fig. 14 (a) and Fig. 15 (a)), the influence of illumination change on the flow and the manometric height is considerable.

Fig. 16 show the volume of the water pumped into the tank. We realize that the water volume increase linearly and is not affected by the transitory variations of the flow at the different points of illumination change, independently of the rotor inertia moment (J) value.

4. Conclusion

This work presents an approach for improving the performances of a direct coupled photovoltaic water pumping system using a centrifugal pump driven by a three-phase asynchronous motor working at fixed speed. We have studied the influence of the rotor

inertia moment J on the performances of the centrifugal motor-driven pump in dynamic regime.
The simulation results show that the diminution of J (or the mechanic power of motor-pump) allowed the minimization of operating disturbances in presence of sudden and important change of illumination. It has been concluded that the dynamic performances of the motor-driven pump improve when its power decreases. It shows also that the volume evolution of the water stocked in the tank is not affected by the illumination variations.

References

[1] D. Mezghanni, R. Andoulsi, A. Mami and D. Dauphin-Tanguy, "Bond Graph Modeling of a Photovoltaic System Feeding an Induction Motor-Pump", Simulation Modeling Practice and Theory, 15: 1224-1238, 2007. https://doi.org/10.1016/j.simpat.2007.08.003.

[2] S. S. Chandel, M. Nagaraju Naik, and Rahul Chandel, "Review of Solar Photovoltaic Water Pumping System Technology for Irrigation and Community Drinking Water Supply", Renewable and Sustainable Energy Reviews, 49: 1084-1099, 2015. https://doi.org/10.1016/j.rser.2015.04.083.

[3] S. R. Baht and al, "Performance Optimization of Induction Motor-Pump using Photovoltaic Energy Source", IEEE Trans. Ind. App., vol. 23, no. 6, pp. 995-1000, 1987. https://doi.org/10.1109/TIA.1987.4505020.

[4] M. Mackhlouf, F. Messai and H. Benalla,"Vectorial Command of Induction Motor Pumping System Supplied by a Photovoltaic Generator", Journal of Electrical Engineering, vol. 62, no. 1, pp. 3-10, 2011. https://doi.org/10.2478/v10187-011-0001-7.

[5] K. Ishaque, Z. Salam, H. Taheri, "Accurate Matlab/Simulink PV System Simulator based on a Two-Diode Model ", Journal of Power Electronics; vol. 11, No. 2, pp. 179-187, 2011. https://doi.org/10.6113/JPE.2011.11.2.179.

[6] B. Bhandari, S. R. Poudel, K-T. Lee and S-H. Ahn,"Mathematical Modeling of Hybrid Renewable Energy System : A Review on Small Hydro-Solar-Wind Power Generation", International Journal of Precision Engineering and Manufacturing-Green Technology, vol. 1, No 2, pp. 157-173, 2014. https://doi.org/10.1007/s40684-014-0021-4.

[7] S. Baig, Prof K. Gupta, "Performance of Mathematical Modeling of Photovoltaic module with Simulink Buck-Boost Converter", International Journal of Engineering Sciences & Research Technology (IJESRT), ISSN: 2277-9655, Vol. 4, No. 6, pp. 722-726, 2015.

[8] M. Villalva, J. Gazoli and E. Filho, "Comprehensive Approach to Modeling and Simulation of Photovoltaic Arrays", IEEE Trans. Power Electron., vol. 24, no. 5, pp. 1198–1208, May 2009. https://doi.org/10.1109/TPEL.2009.2013862.

[9] V. V. Remana, D. Jena and member IEEE, "An Accurate Modeling of Photovoltaic System for Uniform and Non-Uniform Irradiance", International Journal of Renewable Energy Research, vol. 5, no. 1, pp. 29-40, 2015.

[10] H. Abbes, H. Abid and K. Loukil, "An Improved MPPT Incremental Conductance Algorithm Using T-S Fuzzy System for Photovoltaic Panel", International Journal of Renewable Energy Research, vol. 5, no. 1, pp. 160-167, 2015.

[11] V. Salmi, M. Bouzguenda, A. Gastli and A. Masmoudi, "MATLAB/Simulink Based Modelling of Solar Photovoltaic Cell", International Journal of Renewable Energy Research, vol. 2, no. 2, pp. 213-218, 2012.

[12] Prof S. Umashankar, K. P. Aparna, R. Priya and S. Suryanarayanan, "Modeling and Simulation of a PV System Using DC-DC Converter", International Journal of Latest Research in Engineering and Technology (IJLRET), ISSN: 2454 - 5031, vol. 1, issue 2, pp. 09-16, 2015.

[13] T. Raj and R. Ramesh, "Modeling and Analysis of Parallel Converter for Photovoltaic Applications", Journal of Theoretical and Applied Information Technology, ISSN: 1992 – 8645, E-ISSN: 1817-3195, vol. 62, no. 2, pp. 309-316, 2014.

[14] D. Kumard, L. Shaheer, S. Jannat, H. Tamzid, A. Shahriar and R. Jakaria, "Performance Analysis of Boost Inverter for Photovoltaic System", Internationnal Journal of Emerging Technologies in Sciences and Engineering, vol. 5, Nº2, Dec 2011.

[15] M. Vitorino, M. Corrêa, C. Jacobina and A. Lima,"An Effective Induction Motor Control for Photovoltaic Pumping", IEEE Trans. Ind. Electron., vol. 58, no. 4, pp. 1162–1170, Ap. 2011. https://doi.org/10.1109/TIE.2010.2054053.

[16] J. Sun and H. Gotstollen, "Averaged Modeling of Switching Power Converter: Reformulation and Theoretical Basis", IEEE PESC'92, 1166-1172, 1992.

[17] I. Vechiu, "Modeling and Analysis of Renewable Energy Integration in an Autonomous Grid", Ph.D Thesis in electrical engineering, University of Havre, 2005.

[18] V. F. Pires and F. A. Silva, "Teaching Nonlinear Modeling, Simulation, and Control of Electronic Power Converters Using MATLAB/SIMULINK.", IEEE Transaction on education, vol. 45, no. 3, pp.253-261, 2002. https://doi.org/10.1109/TE.2002.1024618.

[19] M. Arrouf, and S. Ghabrour,"Modeling and Simulation of a pumping System fed by Photovoltaic Generator within the Matlab/Simulink Programming Environment",Desalination, 209, pp. 23-30, 2007. https://doi.org/10.1016/j.desal.2007.04.004.

[20] M. F.Mimouni, M. N. Mansouri, B. Benganem and M. Annabi, "Vectorial Command of an Asynchronous Motor Fed by a Photovoltaic Generator", Renewable Energy, Vol. 29, N°3, pp. 433-442, 2004. https://doi.org/10.1016/S0960-1481(03)00226-X.

[21] H. Suehrcke, J. Appelbaum and B. Reshef, "Modelling a Permanent Magnet DC Motor/Centrifugal Pump Assembly in a Photovoltaic Energy System", Solar Energy, 59(1–3): 37–42, 1997. https://doi.org/10.1016/S0038-092X(96)00117-X.

[22] M. Alonso Abella, E. Lorenzo and F. Chenko, "PV Water Pumping Systems Based on Standard Frequency Converters", Progress in Photovoltaic: Research and Applications, 11:179–191, 2003 https://doi.org/10.1002/pip.475.

[23] "Asynchronous Motors data sheet", Leroy Somer, France www.leroy-somer.com/_popup/en/downloads/catalogues/?id=2571.

Appendix

Apparatus	Parameters
PV Array	Type: JS180W-36M Number of series module (N_s): 8 Number of parallels module (N_p): 26
Boost Converter	Output voltage (V_{sh}): 500 V
PI Controller	Référence voltage (V_{ref}): 500 V K_p=0.004; K_i=13 and τ= 10^{-4} s
Voltage Inverter	Input voltage (V_{cc}): 500 V_{DC} Three-phase Output voltage: 230 V_{AC} Frequency (f): 50 Hz
Asynchronous Motor	Phase-phase voltage (U): 400 V Frequency (f): 50 Hz Stator resistance (R_s): 0,85 Ω Stator inductance (L_s):14 mH Rotor inductance (L_r): 23 mH Mutual inductance (M): 58 mH Number of pairs of poles (p): 1
Centrifugal Pump	Performances at 2500 tr/mn Nominal flow (Q_n): 100 m^3/h Nominal height (H_n): 90 m Torque coefficient (k): 15 10^{-5} Nm/(rad/s)^2
Storage Tank	Volume (C): 668 m^3 Water reserve (Vol_0): 16 m^3